ingegneria sismica
International Journal of Earthquake Engineering
Anno XLIII - Num. 3 - 2026

Theoretical Analysis on the Optimal Design of Grouting Reinforcement Technical Parameters in the Construction of High-altitude High-Pressure Water-rich Tunnels

Guocai Zhang[1,*], *Guoxun Zhou*[2], *Mingwei Wang*[2], *Kunjie Wang*[2] *and Qiqi Hou*[2]

[1] China First Highway Engineering Co., LTD., Beijing, China
[2] CCCC First Highway Engineering Group 6th Engineering Co., Ltd., Tianjin, China

SUMMARY: *There are problems in the optimization design of grouting reinforcement technology parameters for high-altitude high-pressure water rich tunnels, such as the selection of grouting materials, grouting pressure, layout of grouting holes, and control of grouting volume. This article studies the optimization design theory of grouting reinforcement technology parameters in the construction of high-altitude high-pressure water rich tunnels. Taking a water rich section of a tunnel as the research object, the ABAQUS finite element analysis software is used to numerically simulate the curtain grouting process. By comparing the data characteristics under two different working conditions, the regulating effect of grouting reinforcement layer on water inflow rate was explored, and the grouting technical parameters were optimized and adjusted based on simulation results. Experimental data shows that compressing the grouting range to within 4 meters can not only ensure that the permeability ratio meets technical requirements, but also significantly reduce material consumption costs. On this basis, a practical and feasible implementation plan for curtain grouting was ultimately formulated. The research results can provide reference for the construction of deep buried, high-pressure, and water rich tunnels. This study will provide theoretical basis for the optimization design of grouting reinforcement technology parameters in the construction of high-altitude high-pressure water rich tunnels, and provide guidance for related engineering design, construction, and management work.*

KEYWORDS: *Grouting Reinforcement; Technical Parameters; Optimal Design; Finite Element Analysis; Curtain Grouting; Numerical Simulation*

1 Introduction

The complex geological conditions faced in the construction of high-altitude high-pressure water-rich tunnels pose severe challenges to traditional construction techniques. The special tectonic movements and climatic characteristics in plateau areas often lead to multiple problems such as enriched aquifers, high permeability of strata and fragmented surrounding rock structures during tunnel excavation [1, 2]. These geological conditions are highly likely to cause sudden water gusps and instability of surrounding rocks, seriously threatening construction safety and increasing engineering risks. Grouting reinforcement technology can significantly enhance the impermeability and mechanical strength of rock mass by injecting grout into the fissures of surrounding rock to form a consolidated body. The core principle lies in that the slurry diffuses and fills the fissures under pressure, forming a continuous water-

*15539074306@163.com
https://doi.org/10.65102/is20261208
Published: 10 June, 2026

blocking curtain and simultaneously enhancing the overall rigidity of the rock mass [3]. The coordinated control of parameters such as the physical and chemical properties of grouting materials, the spatio-temporal distribution of grouting pressure, and the diffusion range of grout directly affects the engineering effect. Parameter optimization design needs to comprehensively consider multi-objective constraints such as geological conditions, construction techniques and environmental effects. In high-altitude and cold regions, the setting time of the slurry is prolonged under low-temperature conditions, and the proportion of admixtures needs to be adjusted to ensure early strength. The difference in permeability coefficients in the water-rich section leads to uneven slurry diffusion, and a dynamic pressure regulation model needs to be established. In addition, the impact of grouting on the groundwater environment cannot be ignored. The fluoride ions and calcium ions released during the solidification process of cement-fly ash slurry may change the chemical composition of groundwater. It is necessary to control the dosage and proportion of slurry to achieve controllable environmental risks. Numerical simulation technology provides important support for parameter optimization.

In high-altitude high-pressure water-rich tunnel projects, the optimization of grouting reinforcement technology plays a crucial role in ensuring construction quality, enhancing operational safety, and reducing ecological impacts [4]. At present, the application of cement-based grouting materials in tunnels of water-rich fault zones has become a key topic of discussion in the academic circle. Taking Zhu Caiwen's research as an example, for tunnel projects with poor stability of surrounding rock, a polyurethane-inorganic composite grouting system was used to reinforce the rock mass. Through systematic testing of the flow characteristics, solidification time and uniaxial compressive performance of the slurry, it was found that there was a significant correlation between the content of polyurethane and the performance of the slurry [5]: an increase in concentration would lead to a decrease in fluidity, a reduction in the diffusion range and an acceleration in the solidification speed. Sun Tieyi focused on the instability problem of weak surrounding rock in the Liaoxi Tunnel. By comparing the flexural and compressive properties of different grouting materials, he revealed the mechanical behavior laws of the materials under different curing cycles, providing an important reference for similar projects. In addition, Liu Yongchao's team conducted systematic tests on various leak-stopping materials such as Mali powder, water-reactive polyurethane, and two-component slurry, deeply analyzed the water-stopping effects and mechanisms of action of each type of material, and based on this, put forward optimization suggestions.

However, at present, some grouting materials have problems such as complicated construction techniques and insufficient stability, which seriously restrict the actual effect of tunnel waterproofing reinforcement. Although some chemical grouting materials can overcome these shortcomings, their environmental hazards are relatively large. Based on this, the development of new grouting materials with excellent stability, outstanding waterproof performance, significant self-healing ability, good consolidation characteristics, superior impermeability and environmental friendliness has become an urgent need in the field of tunnel waterproofing engineering. Due to these outstanding properties, the importance of new polymers in waterproof grouting applications is increasing day by day. However, due to the factor of raw material prices, in order to balance economic efficiency and grouting quality, this study, relying on a tunnel project in a certain area, focuses on discussing key parameters such as the permeability characteristics and reasonable thickness of the tunnel grouting reinforcement layer under water-rich geological conditions through a series of grouting tests combined with numerical simulation.

2 Project Overview and geological Conditions

2.1 Project Overview

The project involves the construction of a newly-built d1200 sewage pipeline approximately 2.8 kilometers long. This pipeline is located beneath the non-motorized vehicle lane on the road, just 1 meter away from the side strip [6]. The designed burial depth of the pipeline is 5 to 18 meters. Along the way, it needs to pass through slightly dense fine sand, soft plastic silty clay, pebble layers, as well as strongly weathered sand rock layers in some local areas. To retain and utilize the existing water supply and stormwater pipelines to the greatest extent and reduce the workload of demolition, the entire sewage pipeline is jacking with a slurry balance shield machine. When pipe jacking passes through sand layers, due to the easy liquefaction property of sand and soil, construction disturbances are prone to cause quicksand phenomena, leading to soil instability. In addition, occasional factors such as over excavation or misalignment of the tunnel boring machine during the excavation process may lead to stratum loss, thereby altering the stress distribution of the soil around the pipeline, causing deformation of the soil around the pipeline, and imposing additional stress and settlement effects on the existing pipelines and the surface within the soil range [7]. To ensure the safety of existing roads and pipelines and guarantee the smooth progress of pipe jacking construction, grouting pre-reinforcement measures are adopted for sections with fine sand layers. Before reinforcement, the optimal grouting parameters are determined through grouting tests.

2.2 Geological Conditions

The lithology of the strata within the exploration depth range of the proposed project site is the Quaternary Holocene (Q4), based on the significant differences in the genesis types, structural features, soil properties and physical and mechanical properties of each soil layer [8].

The fine sand layer that the pipe jacking passes through is grayish yellow to yellowish brown, slightly dense and saturated, mainly composed of powder and sand particles. The particles are well rounded and contain a small amount of sticky particles. The sorting property is medium. Particles larger than 0.075mm account for about 60% of the total mass, those larger than 0.25mm account for about 15%, and those larger than 0.5mm account for about 5%. It shows that the soil quality is relatively uniform. The average number of hits in the measured standard penetration test (SPT) was 11.2. The confined water within the site is mainly distributed in the layers of fine sand and pebbles. Its replenishment mainly comes from the lateral and cross-flow replenishment of the Xinjiang River in Jiangxi Province. The discharge route is the same as the replenishment, and the water volume is relatively abundant. The groundwater level is 2.8 to 6.8 meters below the surface.

(1) Surface water system conditions. No perennial water bodies were found in the project area. Only seasonal runoff occurred in some gullies.

(2) Characteristics of the groundwater system. According to the differences in water-bearing media, they can be classified into two types: bedrock fissure aquifers and Quaternary pore aquifers.

1) Bedrock fissure aquifer. This aquifer mainly exists in the fracture network of fine-grained amphiflash black cloud granodiorite, and its water-richness is jointly restricted by the distribution range of the rock mass and the degree of fracture development. Due to the strong downward cutting of the Yarlung Zangbo River, the groundwater level in the tunnel site area is buried at a relatively deep depth, and atmospheric precipitation constitutes its main source of replenishment.

2) Quaternary pore aquifers. This type of groundwater is mainly stored in sandy sedimentary

layers containing silty clay, and its recharge pathways include local surface water infiltration and atmospheric precipitation recharge.

3 Numerical model of grouting reinforcement

3.1 Construction Preparation

To ensure the smooth implementation of the tunnel grouting reinforcement project and achieve the expected results, it is necessary to complete all the preparatory work in advance in accordance with the design plan. The main preparatory work includes the following aspects [9]:

(1) Conduct operational status checks on the key equipment of the grouting system, with a focus on verifying the working performance of the two-liquid grouting pump, cement conveying device and primary mixing equipment to ensure normal mechanical operation. At the same time, it is necessary to check whether the grouting pipeline and the water supply pipeline are blocked to ensure the stable supply of grout and water source.

(2) Carry out measurement and positioning work to accurately mark the position of the borehole. According to the requirements of the construction drawings, marking and layout are carried out on the working surface to precisely determine the position of each grouting hole. Complete the point position review and numbering work to ensure that the hole position layout complies with the design requirements and the coordinates are correct.

(3) Verify the smoothness of power supply and communication lines to ensure that drainage and sewage facilities are in normal working condition.

3.2 Drilling Construction Process

3.2.1 Determine the drilling parameters and install the grouting pipe at the hole opening

Before carrying out drilling operations, all technical parameters must be carefully checked. The initial diameter of the borehole is set at 150 millimeters, and the depth range is controlled between 2.5 and 4.0 meters. When encountering strata rich in water and with soft geology, to prevent groundwater from gushing out due to grouting pressure and causing damage to the borehole, an appropriate grouting casing should be selected as the hole opening protection device. This casing should have good waterproof performance and structural stability [10]. It is recommended to choose a 145-millimeter diameter steel pipe as the hole opening pipe. This specification can effectively prevent cracks or deformations at the hole opening. The outer wall of the casing needs to be sealed and reinforced with fast-setting cement. After the cement reaches the designed strength, a pressure test of 6 megapascals must be conducted to ensure that the casing is not loose and the sealing performance meets the standards. After the acceptance is qualified, install a valve on the top of the casing and fasten it with bolts. After completing these preparatory works, move the drilling rig to the No. 1 pile position, select an 80-millimeter drill bit, adjust parameters such as the propulsion pressure and drill pipe speed, and only then can the formal drilling operation begin.

3.2.2 Install the anti-protrusion device for drilling

During drilling operations, if no protective measures are taken when the drilling tools pass through water-bearing and soft strata, high-pressure mud will rapidly seep into the interior of the tunnel and, under the effect of pressure difference, form a gushing phenomenon from bottom to top, eventually leading to the complete failure of the borehole. For drilling projects in water-rich and weak strata, technical solutions for preventing seepage and gushing must be pre-

deployed [11]. One of the common practices is to pre-embed protective casing before drilling commences. This type of casing usually selects steel pipes with a diameter slightly smaller than the designed hole diameter, and it has the comprehensive functions of preventing leakage, resisting gushing and stabilizing the hole wall. In addition, by using the orifice sealing device and the high-pressure control valve system in combination, and adjusting the pressure balance inside and outside the orifice, the penetration of external mud can be effectively blocked, thereby properly solving the problems of water gushing in the formation and mud eruption.

3.2.3 Drilling and hole formation

Under the condition of ensuring the effective implementation of the above protective measures, the quality of drilling and forming will be significantly improved. When the first drill pipe reaches the predetermined depth, the drill tool should be slowly withdrawn at a uniform speed. Subsequently, the remaining mud debris and rock cuttings in the hole must be thoroughly removed. The acceptance criteria require that the hole wall remain flat and smooth, without obvious cracks and the verticality deviation does not exceed ±1°. If obvious cracks are found on the hole wall or the verticality exceeds the limit value specified in the specification, the hole is regarded as unqualified and the drilling point needs to be repositioned after consultation with the technical personnel. To optimize the construction progress of tunnel grouting reinforcement, a three-dimensional cross-operation plan of drilling and grouting procedures was implemented on site. The construction unit adopts a group of 5 holes. After completing the first group of drilling operations, it immediately proceeds to the grouting process. After the first group of grouting operations is completed, the next group of drilling construction can be carried out. At this time, the materials inside the holes that have been grouted will gradually complete the initial setting, thereby achieving a comprehensive improvement in construction efficiency.

3.3 Numerical Model for Grouting Reinforcement

3.3.1 Finite Element Model

This study adopts numerical simulation methods to conduct grouting construction analysis for tunnel projects under specific geological conditions. By establishing calculation models for different working conditions, the dynamic influence of changes in grouting parameters on the grouting effect of the curtain is mainly discussed. During the research process, the interaction mechanism among the seepage characteristics around the tunnel, the displacement features of the rock mass and the evolution law of the plastic zone was systematically investigated [12].

A three-dimensional model of the tunnel was established using the finite element software ABAQUS, with model dimensions of 100m × 100m × 50m. Among them, the maximum height of the model is 100 meters. The surface of the model is simulated based on actual terrain conditions. The grid cells are linear and composed of tetrahedral C3D4P. The constitutive model is an ideal elastoplastic Moorn-Coulomb model, as shown in Figure 1.

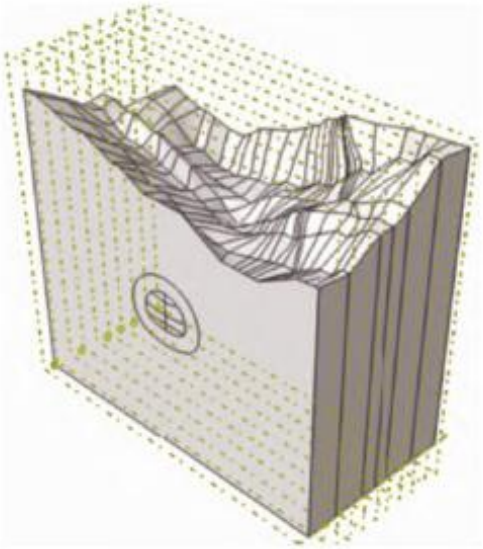

Figure 1: Tunnel model

The basic mechanical property parameters of the material are as follows: the mass per unit volume is 2.5 tons per cubic meter, the elastic deformation modulus is 6GPa, the lateral deformation coefficient is 0.25, the shear failure Angle is 50°, the shear strength parameter is 0.7MPa, and the hydraulic conductivity is 3.06×10-5m/h. These values are consistent with the on-site geological exploration data [13].

The constraint conditions for numerical simulation are set as follows: In the processing of displacement boundaries, a fixed constraint method is adopted, specifically restricting the horizontal displacement of the left and right boundaries and the vertical displacement at the bottom, while only retaining the free deformation at the top. For the seepage boundary, permeable boundary conditions are set at the bottom and surrounding areas of the model to simulate the replenishment or discharge process of karst fissure water to the calculated area. The area within 5 meters around the tunnel is the grouting reinforcement zone, and its geometric shape is shown in Figure 2.

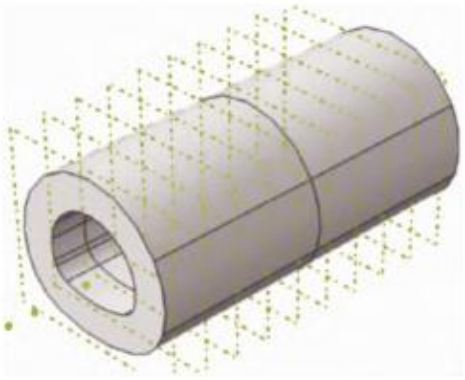

Figure 2: Grouting ring model

3.3.2 Grouting Model Analysis

This paper mainly analyzes two working conditions: no grouting and full-section curtain grouting. Under the no grouting condition, the parameters of the grouting reinforcement ring are the same as those in the surrounding rock. The following formula for the diffusion range of

grout can be used to analyze the grouting effect:

$$R = \sqrt{\frac{2k \cdot p \cdot t}{\mu \cdot \beta}} \tag{1}$$

where, R is the diffusion radius, k is the permeability, p is the injection pressure, t is the injection time, μ is the viscosity of the slurry, and β is the volume ratio of the slurry to water.

When implementing the full-section curtain grouting process, the physical and mechanical parameters of the grouting ring are configured as follows: The material density is set at 2.6t/m³, the elastic deformation modulus reaches 6.1GPa, the lateral deformation coefficient is taken as 0.2, the internal friction Angle in the shear strength parameters is 41 degrees, the bonding strength value is 800kPa, and the fluid permeability performance index is 3.06×10-6m/h.

(1)Analysis of pore water pressure results

Based on the results of numerical simulation calculations, a special study was carried out on the excavation process of the 25-meter section in the middle of the tunnel, with a focus on investigating the stress distribution and seepage characteristics of this area. When analyzing the distribution of pore water pressure, the following formula for pore water pressure distribution can be used:

$$p = \gamma_w \cdot h \tag{2}$$

where, p is the pore water pressure, is the density of water, and h is the head height.

The data in Figure 3 shows that when no grouting measures are taken, within a 5-meter range of tunnel excavation, the peak pore water pressure occurs 5 meters below the tunnel floor, with a value reaching 0.147MPa. After the implementation of full-section grouting reinforcement with a thickness of 5m, the maximum pore water pressure was transferred to the bottom position of the grouting circumferential reinforcement area, and its value increased to 0.155MPa. This phenomenon indicates that although the full-section grouting process increases the pore water pressure of the surrounding rock, it effectively blocks the infiltration channel of fissure water into the tunnel interior, thereby verifying the actual effect of the grouting reinforcement technology.

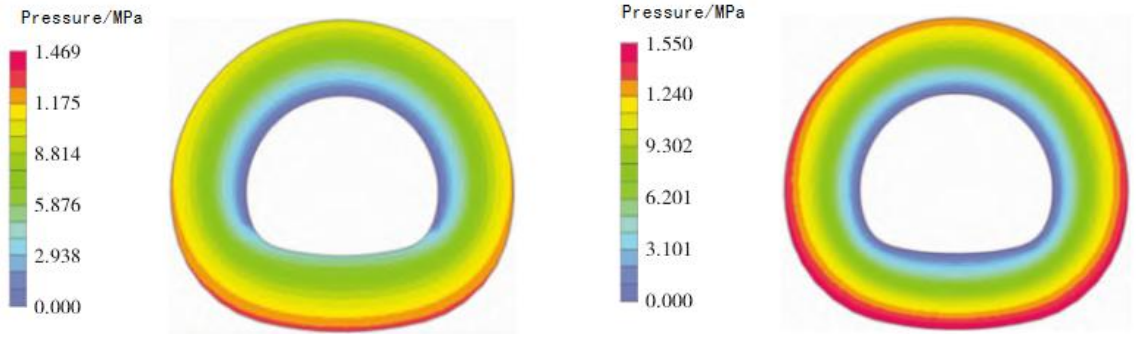

(a)no grouting (b)During grouting

Figure 3: Distribution of pore water pressure within a 5-meter range of tunnel excavation

(2) Analysis of seepage velocity results

Figure 4 shows the spatial distribution characteristics of the flow velocity vector. Observation reveals that regardless of whether the grouting process is implemented or not, the peak flow rate of water gushing in the tunnel always occurs in the arch foot area. This phenomenon shows significant consistency under both working conditions. Without grouting,

the maximum flow velocity measured was 1.560×10-4m/s. After the implementation of full-section curtain grouting, this value dropped to 1.395×10-5m/s. Data comparison shows that the adoption of full-section curtain grouting technology can significantly reduce the peak flow of water gushing in tunnels by an order of magnitude. This phenomenon confirms the effectiveness of the grouting process in controlling the flow rate of water gushing and has a significant waterproofing effect on tunnel construction. Select the flow velocity parameters from the top of the arch to the bottom of the left wall and then to the arch bottom area, and draw the flow velocity distribution trend chart as shown in Figure 5. As can be seen from the analysis of Figure 5, the seepage velocity curve under the condition of no grouting shows obvious peak characteristics, indicating that there are severe flow velocity fluctuations in the arch foot area. This unstable seepage state will have an adverse effect on the lining structure. In contrast, the flow velocity curve changes more gently under the condition of full-section curtain grouting. This stable flow characteristic helps maintain the integrity of the lining structure. Based on the above analysis results, this study selects the full-section curtain grouting scheme for the subsequent parameter optimization work.

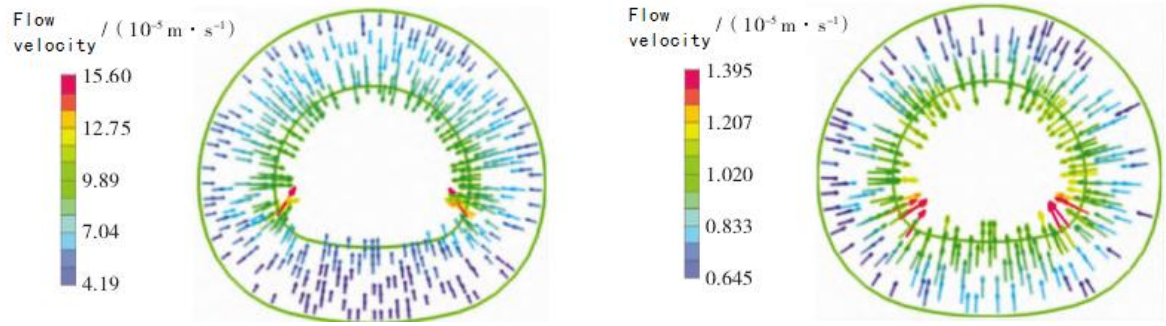

(a)no grouting (b)Full-section curtain grouting

Figure 4: Flow velocity vector

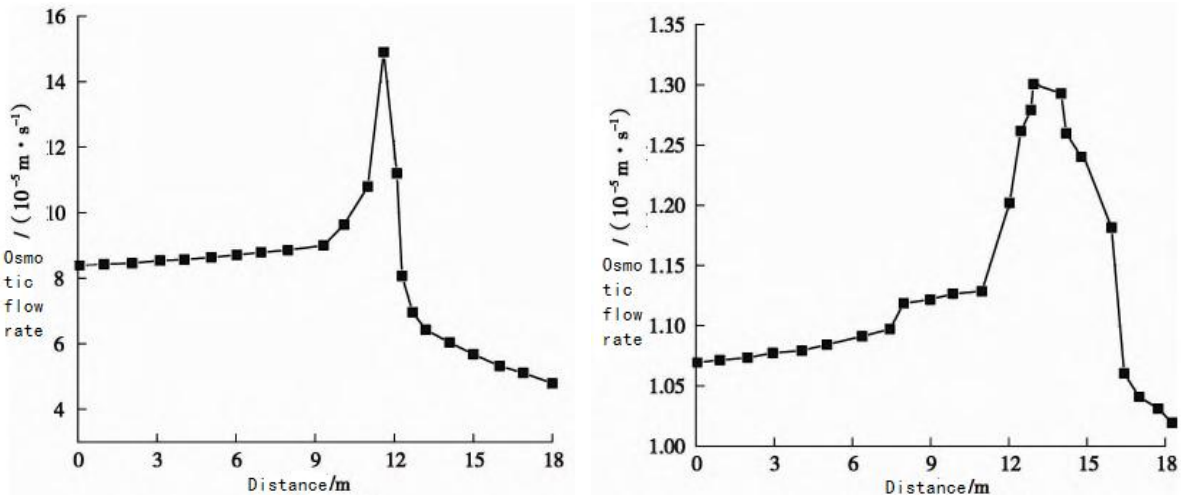

(a)no grouting (b) Full-section curtain grouting

Figure 5: Flow velocity curve

4 Key technical Parameters for Grouting reinforcement

4.1 Thickness of grouting ring

The thickness design of the grouting ring has a decisive influence on the mechanical response of the tunnel surrounding rock and the support system [14, 15]. It can not only improve the load-bearing performance of the structure, but also effectively prevent the infiltration of groundwater, thereby significantly changing the displacement distribution and seepage characteristics of the surrounding rock area [16]. Based on this, this study conducted numerical simulation analysis of the deformation characteristics of surrounding rock for six different thicknesses of grouting rings (1m, 2m, 3m, 4m, 5m, 6m) within the range of 1 meter to 6 meters. Figure 6 shows the deformation law curves of the tunnel surrounding rock under different thicknesses of the grouting layer.

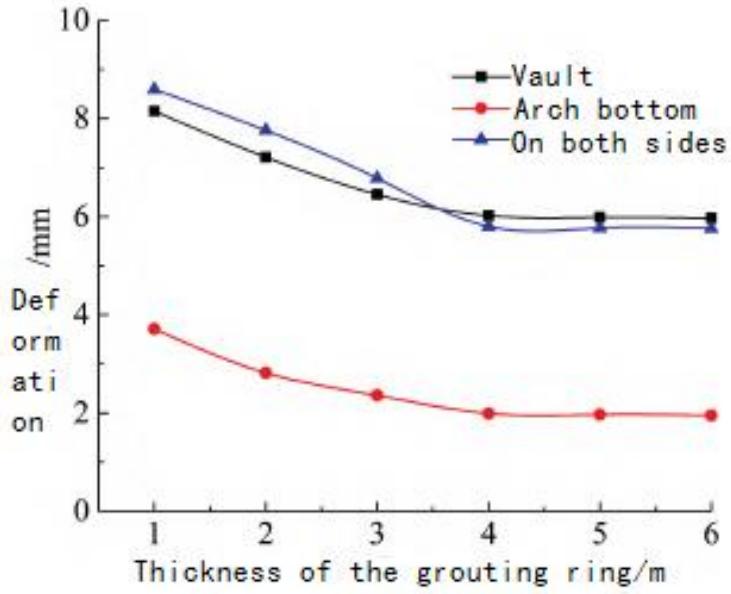

Figure 6: Deformation curves of tunnel surrounding rock under different thicknesses of grouting rings

Figure 6 shows that as the thickness of the grouting ring gradually increases, the settlement at the top of the tunnel arch, the uplift at the bottom of the arch, and the deformation on both sides all show a decreasing trend. When the thickness of the grouting ring reaches 1 meter, the settlement at the top of the arch is 8.15 millimeters, the uplift at the bottom of the arch is 3.71 millimeters, and the deformation on both sides is 8.59 millimeters. The formula for calculating deformation is as follows:

$$\Delta S = S_0 - S_i \tag{3}$$

where, S_0 is the initial settlement amount, and S_i is the settlement amount at different thicknesses.

When the thickness of the grouting ring was increased to 2 meters, 3 meters, 4 meters, 5 meters and 6 meters, compared with the thickness of 1 meter, the settlement at the top of the arch, the uplift at the bottom of the arch and the deformation on both sides were reduced by 11.5%, 23.9% and 9.6% respectively. 20.8%, 36.3% and 21.0%; 26.1%, 46.3% and 32.4%; 26.5%, 46.9% and 32.8%; 26.7%, 47.4% and 32.9%. The increase in the thickness of the

grouting ring continuously reduces the deformation of the surrounding rock. However, when the thickness exceeds 4 meters, the variation range of the surrounding rock displacement slows down significantly, and the deformation control effect no longer improves significantly. From an economic perspective, 4 meters is the best thickness choice for the grouting ring. When analyzing the economy, the following economic optimization formula can be used:

$$C = \alpha \cdot T + \beta \cdot P \tag{4}$$

where, C is the total cost, T is the thickness of the grouting layer, P is the permeability ratio, and α and β are the weight coefficients.

Table 1 presents the statistical results of deformation of tunnel surrounding rock at different thicknesses.

Table 1: Statistical results of deformation of tunnel surrounding rock under different thicknesses

Thickness (m)	Crown settlement (mm)	Arch bottom uplift (mm)	Deformation on both sides (mm)
1	8.143	3.608	8.59
2	7.148 (-11.53%)	2.831 (-20.82%)	7.658 (-9.64%)
3	6.109 (-23.92%)	2.227 (-36.31%)	6.417 (-21.05%)
4	5.875 (-26.14%)	1.870 (-46.33%)	5.650 (-32.46%)
5	5.864 (-26.55%)	1.865 (-46.89%)	5.632 (-32.83%)
6	5.849 (-26.71%)	1.829 (-47.46%)	5.621 (-32.92%)

From the data in Table 1, the influence of different thickness grouting rings on the deformation of tunnel surrounding rock can be analyzed in depth. When the thickness of the grouting ring increases from 1 meter to 2 meters, the settlement of the arch crown decreases from 8.143mm to 7.148mm, a decrease of 11.53%; The arch bottom lift decreased from 3.608mm to 2.831mm, a decrease of 20.82%; The deformation on both sides decreased from 8.59mm to 7.658mm, a decrease of 9.64%. This indicates that the 2-meter thick grouting ring has a certain control effect on the deformation of the surrounding rock, but the effect is not yet significant. When the thickness increases to 3 meters, the settlement of the arch crown drops to 6.109mm, a decrease of 23.92%; The arch bottom was lifted to 2.227mm, a decrease of 36.31%; The deformation on both sides decreased to 6.417mm, a decrease of 21.05%. Compared with a thickness of 2 meters, the deformation control effect has been significantly improved, indicating that the 3-meter-thick grouting ring has a significantly enhanced inhibitory effect on surrounding rock deformation.

When the thickness reaches 4 meters, the settlement of the arch crown drops to 5.875mm, a decrease of 26.14%; The arch bottom was lifted to 1.870mm, a decrease of 46.33%; The deformation on both sides decreased to 5.650mm, a decrease of 32.46%. Compared with a thickness of 3 meters, although the reduction in deformation still increases, the amplitude has decreased. When the thickness exceeds 4 meters, such as 5 meters and 6 meters, the decrease in settlement of the arch crown, uplift of the arch bottom, and deformation on both sides changes slightly. This indicates that when the thickness of the grouting ring exceeds 4 meters, the range of displacement changes in the surrounding rock significantly slows down, and the deformation control effect is no longer significantly improved. Combining the economic optimization formula and considering both cost and deformation control effects, a 4-meter-thick grouting ring is the best choice as it can effectively reduce costs while ensuring good deformation control.

4.2 Permeability coefficient of grouting ring

When the thickness of the grouting ring is fixed, the change in the permeability coefficient will significantly affect its waterproof performance [17]. This difference in waterproof performance will alter the water flow distribution state of the rock mass around the tunnel, thereby exerting varying degrees of influence on the displacement distribution of the surrounding rock and the load borne by the support system.

First, define. n= k1/k2, where k1 is the permeability coefficient of the surrounding rock of the tunnel before grouting, and k2 is the permeability coefficient of the grouting ring after the tunnel is reinforced by grouting. The thickness of the grouting ring was selected as 4 m, and the water inflow per meter of the tunnel under the conditions of permeability ratio n=1, 2, 5, 10, 30, 50, 70, and 100 was studied respectively. The variation curves of water inflow in the tunnel under different permeability ratios are shown in Figure 7.

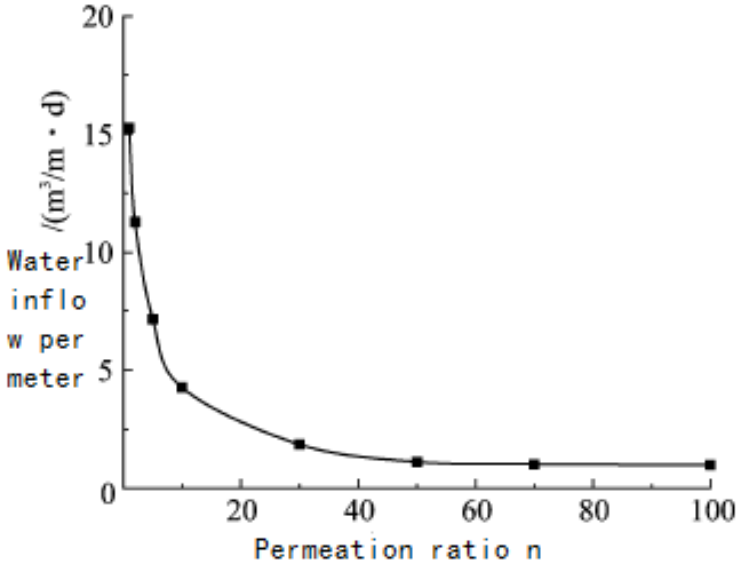

Figure 7: shows the variation curves of water inflow in tunnels with different permeability ratios n

As can be seen from the data in Figure 7, when the permeability ratio n=1, that is, when the permeability coefficients of the surrounding rock of the tunnel and the grouting ring are equal, the water inflow per meter of the tunnel reaches 15.26m³/d, and at this time, the water-stopping effect is at the lowest level. With the continuous increase of the permeability ratio n value, the water inflow in the roadway shows a decreasing trend, and the grouting water-stopping effect is enhanced accordingly. Specific data shows that when the n values are taken as 2, 5, 10, 30, 50, 70, and 100 respectively, the water inflow per unit length of the tunnel decreases by 26.1%, 53.0%, 72.0%, 87.8%, 92.7%, 93.3%, and 93.5% respectively compared to the benchmark value of n=1. It is worth noting that when the permeability ratio exceeds 50, the rate of change in water inflow significantly decreases, and the curve trend tends to stabilize. At this point, the improvement in the grouting water blocking effect is no longer obvious. Considering the economic aspect comprehensively, the reasonable value of the permeability ratio is 50.

Table 2 shows the statistical results of water flow per unit length of the tunnel under different permeability ratios.

Table 2: Statistics of Water Flow per Unit Length of Tunnel under Different Penetration Ratios

Penetration ratio (n)	Water flow rate (m^3/d)	Reduction ratio (%)
1	15.254	0
2	11.265	26.135
5	7.164	53.078
10	4.265	72.056
30	1.886	87.890
50	1.109	92.758
70	1.021	93.331
100	1.005	93.583

The data in Table 2 can provide a deeper analysis of the impact of permeability ratio on the water flow rate per unit length of the tunnel. When the permeability ratio n=1, that is, the permeability of the tunnel surrounding rock and the grouting ring is the same, the water flow rate per unit length of the tunnel is 15.254m ³/d. This indicates that in this state, the grouting ring basically does not play a water stopping role, and the water flow rate is at a high level. As the permeability ratio n gradually increases, the water flow rate shows a significant decreasing trend. When n increases to 2, the water flow rate drops to 11.265m ³/d, a decrease of 26.135% compared to n=1. This indicates that a slight increase in permeability ratio allows the grouting ring to begin to exert a certain waterproofing effect, effectively reducing water flow.

When the permeability ratio n increases to 5, the water flow rate further decreases to 7.164m ³/d, with a reduction rate of 53.078%. Compared with n=2, the decrease in water flow rate significantly increases, indicating that the waterproofing effect of the grouting ring is significantly enhanced with the increase of permeability ratio. When the permeability ratio n reaches 10, the water flow rate is only 4.265m ³/d, with a reduction rate of up to 72.056%, further highlighting the waterproof effect of the grouting ring. However, when the penetration ratio exceeds 50, the trend of change shows a turning point. When n=50, the water flow rate is 1.109m ³/d, with a reduction ratio of 92.758%; When n increases to 70 and 100, the water flow rates are 1.021m ³/d and 1.005m ³/d, respectively, with a reduction ratio of 93.331% and 93.583%, respectively. It can be seen that after the permeability ratio exceeds 50, the reduction in water flow rate slows down significantly, and further increasing the permeability ratio has limited effect on further reducing water flow rate. Taking into account both the waterproofing effect and cost, a permeability ratio of 50 is more reasonable.

4.3 The Influence of Surrounding Rock permeability coefficient

When analyzing the seepage characteristics after tunnel excavation, the influence law of the variation of the permeability coefficient of the surrounding rock on the seepage velocity was mainly investigated [18]. The study set up a 5-meter-thick grouting reinforcement area for comparative analysis with the unreinforced area. Based on the numerical simulation results, three representative sets of permeability coefficient data were selected: 3.05×10-5m/h, 1.2×10-6m/h and 2.55×10-7m/h. Figure 8 shows the variation trend of seepage velocity with the permeability coefficient of surrounding rock under the condition that the thickness of the grouting reinforcement layer is 5 meters. Experimental data show that the seepage velocity is positively correlated with the permeability coefficient of the surrounding rock. Meanwhile, the seepage velocity in areas without grouting measures is significantly higher than that in areas that have undergone grouting treatment. When analyzing the relationship between seepage velocity and permeability, the following formula for calculating water flow rate can be used:

$$Q = A \cdot v \tag{5}$$

where, Q is the water flow rate, A is the seepage cross-sectional area, and v is the seepage velocity.

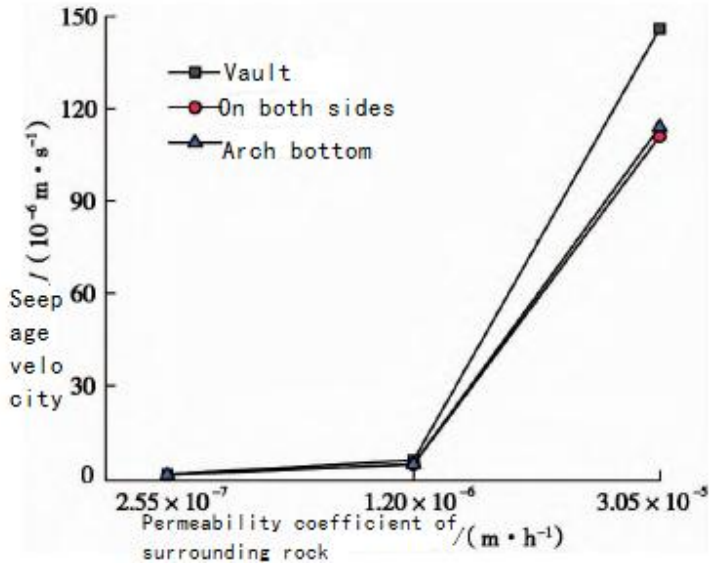

Figure 8: shows the relationship between seepage velocity and the permeability coefficient of surrounding rock

4.4 Curtain grouting reinforcement Scheme

When the length of the construction platform is greater than 10 meters and the slope Angle is less than 300 meters, a 30 cm thick layer of C25 concrete is sprayed on the upper surface of the construction platform for surface hardening treatment [19, 20].

(2) At the position of the grouting wall, dig a groove with a depth of 1 meter and a width of 4 meters along the circumferential direction of the tunnel. Then, build a 4 meter thick grouting wall and embed it 1 meter into the tunnel bedrock in the circumferential direction to enhance the horizontal resistance of the grouting wall.

(3) Before grouting, a drainage hole with a diameter of ϕ130~ should be drilled on each side below the grouting wall as drainage holes. The drainage holes should be arranged at an Angle of 500-700 mm upward (downward), extending 10 meters beyond the grouting area. At the same time, a 125mm steel pipe should be buried in the drainage holes to seal the high-pressure water, with the length of the steel pipe extending 2 meters beyond the grouting area. The position of the grouting holes should be marked on site. A ϕ115mm drill bit was used to drill a hole with a depth of 4.3 m in the stopper rock disk, and a 4.5 m length of ϕ108×4 mm hot-rolled seamless steel pipe was buried as the orifice pipe.

(4) The area for tunnel grouting operations is demarcated within 4 meters outside the excavation contour line. The design adopts a 5-ring grouting hole layout scheme. The total length of a single grouting cycle is 24 meters, and this cycle is divided into three grouting sections: the first section deals with the 0-7 meters area in front of the grouting stop wall, the middle section is responsible for the 7-14 meters range, and the last section covers the 14-21 meters section. After the grouting process is completed, a 16-meter tunneling operation is carried out, and a 5-meter unexcavated section is retained as a stop-grouting barrier for the subsequent grouting cycle.

(5) The grouting material adopts water-soluble polyurethane grouting liquid, which has

good hydrophilicity, large expansion rate and water retention capacity. It can undergo polymerization reaction with water in the presence of a large amount of water. After curing, it forms an impermeable consolidated layer to block water gushing. At the same time, the reaction generates COZ gas pressure, which can drive the grouting slurry to diffuse deep into the fine cracks, fill the pores and fissures of the surrounding rock outside the dense tunnel contour line, and seal the high-pressure water outside the grouting area, preventing the high-pressure water from entering the tunnel contour line.

(6) The grouting material within the tunnel contour line adopts ordinary cement and sodium silicate double slurry, supplemented by ordinary cement grouting, which can reinforce the loose and broken rock mass in front of the tunnel face and prevent collapse during tunnel excavation.

(7) Drilling grouting and drainage pressure reduction are carried out simultaneously. When operating the grouting hole at the upper left corner of the grouting wall, only the drainage hole at the upper left corner of the grouting wall is used for drainage pressure reduction (drilling grouting is conducted at other positions of the grouting wall, and the drainage method is the same). In this way, during the drainage process of the drainage hole, the water in the grouting area can be diverted to the outside of the grouting area. Under the driving effect of the water flow, The grouting pressure was reduced, the grouting range was expanded, and the drainage of the grouting slurry was achieved.

5 Conclusion

The geological structure in the plateau area is special. During the construction of high-pressure water-rich tunnels, the groundwater level is high and the water flow is large, which can easily cause engineering disasters such as water inrush, sand flow and collapse, seriously threatening construction safety. The construction of high-pressure water-rich tunnels on the plateau has put forward strict requirements for the grouting reinforcement process. The effectiveness of grouting reinforcement directly affects the safety, project quality and progress control of tunnel construction. The reasonable optimization of grouting process parameters plays a crucial role in enhancing construction efficiency, saving cost input and ensuring construction safety. In this study, the finite element analysis software ABAQUS was used to conduct numerical simulation calculations for the curtain grouting of rock mass tunnels. Data processing and comparative analysis of the two working conditions show that the grouting reinforcement ring effectively reduces the water gushing speed, thereby significantly improving the seepage control effect. However, it should be noted that although tunnel grouting reduces the water gushing rate, due to the increase in pore water pressure within the reinforcement ring, the grouting reinforcement ring needs to bear greater load pressure. Based on the comprehensive summary of the numerical simulation grouting results and theoretical research, the following grouting scheme optimization was implemented.

When the permeability coefficient ratio increases to 4, the reduction in seepage velocity slows down, indicating that the influence of the coefficient of the grouting reinforcement ring on the seepage velocity is discontinuous. Therefore, a permeability coefficient ratio of 4 is the inflection point of the reduction in seepage velocity. It is more economically reasonable for the permeability coefficient of the grouting ring to be 1/4 of that of the surrounding rock.

(2) When the grouting ring is located within a 4-meter range of the tunnel contour and the permeability ratio is 50, the grouting blocking effect is the most significant. It is suggested that the grouting range be reduced to within 4 meters, which can lower the cost of engineering materials.

As tunnel engineering extends into deeper and more complex strata, the optimization research of grouting reinforcement technology should pay more attention to the cross-

integration of multiple disciplines. In the future, it is necessary to further integrate rock mechanics, fluid mechanics, materials science and information technology to build a full life cycle technology system covering geological prediction, parameter optimization, intelligent construction and health monitoring. Through continuous technological innovation and engineering practice verification, it is expected to provide more targeted and forward-looking technical solutions for the construction of high-altitude high-pressure water-rich tunnels, effectively ensuring the construction safety and long-term stability of tunnel projects under complex geological conditions.

References

[1] Namli M. Evaluation of the effect of using fiber reinforcement in tunnel linings for metro projects[J]. Underground Space, 2021, 6(6): 732-750.

[2] de Andrade G G, de Figueiredo A D, Galobardes I, et al. Experimental and numerical investigation of flexural behavior of precast tunnel segments with hybrid reinforcement[J]. Tunnelling and Underground Space Technology, 2024, 154: 106094.

[3] Wada D, Araujo-Estrada S A, Windsor S. Unmanned aerial vehicle pitch control under delay using deep reinforcement learning with continuous action in wind tunnel test[J]. Aerospace, 2021, 8(9): 258.

[4] Wada D, Araujo-Estrada S A, Windsor S. Unmanned aerial vehicle pitch control using deep reinforcement learning with discrete actions in wind tunnel test[J]. Aerospace, 2021, 8(1): 18.

[5] Goyal R, Mercado A E, Ring D, et al. Most YouTube videos about carpal tunnel syndrome have the potential to reinforce misconceptions[J]. Clinical Orthopaedics and Related Research®, 2021, 479(10): 2296-2302.

[6] Hosseini S M, Mousa S, Mohamed H M, et al. Structural behavior of precast reinforced concrete tunnel segments with glass fiber-reinforced polymer bars and ties under bending load[J]. ACI Structural Journal, 2022, 119(1): 307-319.

[7] Shoeb M, Khan S A, Alam T, et al. Dynamic stability analysis of metro tunnel in layered weathered sandstone[J]. Ain Shams Engineering Journal, 2024, 15(1): 102258.

[8] Mishra S, Zaid M, Rao K S, et al. FEA of urban rock tunnels under impact loading at targeted velocity[J]. Geotechnical and Geological Engineering, 2022, 40(4): 1693-1711.

[9] Hammoud M A, Tuhta S, Günday F. Determination of modal parameters of reinforced concrete tunnel retrofitted with CFRP using finite element method[J]. International Journal of Innovations in Engineering Research and Technology, 2022, 9(4): 10-18.

[10] Zaheri M, Ranjbarnia M, Dias D. New analytical approach to simulate the longitudinal fiberglass dowels performance installed at the face of a tunnel embedded in weak and weathered rock masses[J]. Computers and Geotechnics, 2023, 153: 105080.

[11] Neu G E, Edler P, Freitag S, et al. Reliability based optimization of steel-fibre segmental tunnel linings subjected to thrust jack loadings[J]. Engineering Structures, 2022, 254:

113752.

[12] Shimamoto K, Yashiro K. New rockbolting methods for reinforcing tunnels against deformation[J]. International Journal of Rock Mechanics and Mining Sciences, 2021, 147: 104898.

[13] Trabucchi I, Tiberti G, Plizzari G A. A parametric numerical study on the behavior of large precast tunnel segments during TBM thrust phase[J]. Engineering Structures, 2021, 241: 112253.

[14] Alonso E, Ramon-Tarragona A, Verda L. Designing tunnel lining in anhydritic claystones. Intensity and distribution of swelling forces[J]. Rock Mechanics and Rock Engineering, 2023, 56(2): 1467-1487.

[15] Mehmandari T A, Shokouhian M, Imani M, et al. Experimental and numerical analysis of tunnel primary support using recycled, and hybrid fiber reinforced shotcrete[C]// Structures. Elsevier, 2024, 63: 106282.

[16] Kavvadas M, Georgiou D, Kalos A. Numerical investigation of tunnel face stability using forepoling or fiberglass nails[J]. Geotechnical and Geological Engineering, 2022, 40(2): 843-855.

[17] Goel M D, Verma S, Mandal J, et al. Effect of blast inside tunnel on surrounding soil mass, tunnel lining, and superstructure for varying shapes of tunnels[J]. Underground Space, 2021, 6(6): 619-635.

[18] Hosseini S M, Mousa S, Mohamed H M, et al. Experimental and analytical study on precast high-strength concrete tunnel lining segments reinforced with GFRP bars[J]. Journal of Composites for Construction, 2022, 26(5): 04022062.

[19] Oliveira J M J, Vieira C S, Silva M F A, et al. Fracture modelling of steel fibre reinforced concrete structures by the lumped damage mechanics: Application in precast tunnel segments[J]. Engineering Structures, 2023, 278: 115487.

[20] Sadique M R, Zaid M, Alam M M. Rock tunnel performance under blast loading through finite element analysis[J]. Geotechnical and Geological Engineering, 2022, 40(1): 35-56.